Biomedical Applications and Syntheses of Selected Anthraquinone Dyes

Richard Barry Sirard III

A Senior Thesis submitted in partial fulfillment
of the requirements for graduation
in the Honors Program
Liberty University
Spring 2021

Acceptance of Senior Honors Thesis

This Senior Honors Thesis is accepted in partial
fulfillment of the requirements for graduation from the
Honors Program of Liberty University.

_____
Michael Korn, Ph.D.
Thesis Chair

_____
Abigail Solitro, Ph.D.
Committee Member

_____
Marilyn Gadomski, Ph.D.
Honors Assistant Director

_____
Date

Abstract

Anthraquinones are aromatic organic compounds that have multiple applications in the biomedical field. Some anthraquinone-based compounds are used as fluorophores to contrast cell nuclei while others act as chemotherapeutic agents. However, there are not many fluorescent anthraquinone cell stains currently available. In this study, commercially available anthraquinone dyes, in addition to other dye families and compounds, were reviewed for their unique properties, advantages, and drawbacks. The development and characterization of three novel anthraquinone fluorophores revealed promising photophysical characteristics, like large Stokes shifts. One of the compounds, RBS3, was chosen for fixed and live cell staining and exhibited desirable biomedical properties. RBS3 is highly cell permeable, appears to be photostable, does not require a wash-off procedure, and stains the nucleus, cytoplasm, and endoplasmic reticulum.

Biomedical Applications and Syntheses of Selected Anthraquinone Dyes

■ INTRODUCTION

Anthraquinones are tricyclic organic molecules that form the backbone of several important biomedical compounds. Some anthraquinone-based compounds have unique biological characteristics that allow them to be used as fluorescent dyes. Fluorophores possess the ability to absorb light at various wavelengths and release light at longer wavelengths. This important characteristic allows scientists to more easily visualize cell structures and organelles, such as the nucleus. There are a variety of readily available commercial fluorophores that can stain the nucleus, but each has its advantages and disadvantages. Some common fluorescent dyes are inexpensive and possess high quantum yields, but often demonstrate high photobleaching or narrow Stokes shifts (the latter is commonly seen in rhodamine dyes).[1] An advantage to anthraquinone dyes is that they typically show a higher resistance to photobleaching once substituents have been added.[2]

Anthraquinone derivatives have also been identified and used as cytotoxic agents. Anthraquinones have a planar structure and thus can inhibit vital replication enzymes such as topoisomerase II via binding or intercalating with double-stranded DNA.[3] Because of this ability to inhibit enzymes involved in replication, as well as the capacity to inhibit other upstream targets, anthraquinones have been noted for their ability to induce autophagy.[4] Anthraquinone-derived drugs such as mitoxantrone and doxorubicin are some of the most effective clinical antitumor agents available.[3] Some anthraquinone compounds, such as those isolated from the Rubiaceae plant family, have also been examined for their antimicrobial activity.[5]

This research involved the synthesis and development of anthraquinone-based

compounds in order to examine their biomedical applications. Although there exists a multitude of biomedically relevant molecules that utilize other cores, such as rhodamine and cyanine backbones, there is a relative scarcity of fluorescent compounds utilizing anthraquinone cores. Due to their unique fluorescent characteristics and notable cytotoxic properties, there is a demand for new anthraquinone-based compounds. The primary goal of this research was to develop new anthraquinone derivatives that exhibit unique and desirable photophysical qualities and biomedically relevant characteristics. Three novel compounds were designed in this study to have fluorescent, cell-staining capabilities that would bind to double-stranded DNA (dsDNA). An in-depth understanding of the science behind fluorescence is important when designing and analyzing potentially new fluorescent compounds. Thus, this phenomenon will be further examined.

Fluorescence

The phenomenon of fluorescence was first discovered in the compound quinine by Frederick Herschel in 1845, and further explained later by Sir George Stokes in 1852.[6] Research stagnated until the development of fluorescence microscopy in the 1950s.[6] Since then, research into fluorescence has played a vital role in the development of analytical techniques including the fluorescent labeling of proteins, flow cytometry, fluorescence microscopy, confocal microscopy, and more.

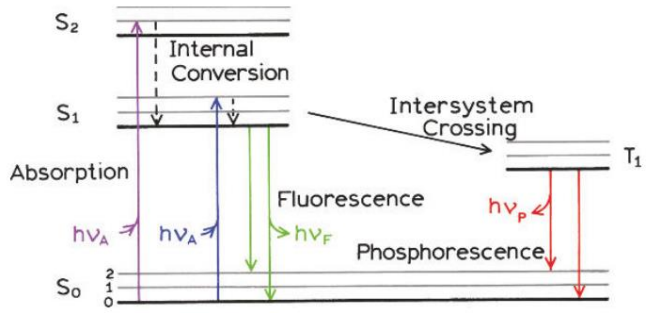

Figure 1. Example of a Jablonski diagram.[7]

Fluorescence occurs when photons excite the electrons of a fluorophore to a higher energy level. When the electrons return to the ground state, the energy is emitted in a form of light, known as fluorescence. The emission rates of fluorescence are extremely rapid; the average time between excitation and emission of a fluorophore is about 10 ns.[7] A Jablonski diagram (Figure 1) visually demonstrates this process of absorbing and releasing light.

When designing and comparing fluorescent molecules, there are several important factors of fluorescence to consider. These factors include the structure of the fluorophore, the absorption and emission maxima, Stokes shift, quantum yield, and photostability. Fluorescence greatly depends on the structure of the fluorophore itself. Typical fluorescent molecules have conjugated π bonds, or a conjugate system, and thus a high number of delocalized electrons. Some, not all, conjugated systems can absorb light and emit the energy as fluorescence. Popular fluorophore cores, such as cyanine, as well as anthraquinone cores are examples of conjugated systems that naturally lend themselves to fluoresce based on their structure. This characteristic depends on the ability of ultraviolet-visible (UV-Vis) light to excite a fluorophore's highest occupied molecular orbital (HOMO) π electron to the π* (antibonding) orbital.[8] The emission of a photon allows direct relaxation of the electron.[8] Based on the importance of π bonds, it is no

surprise that increasing the number of conjugated π bonds or adding functional groups that can donate electrons have an impact on the fluorescence spectra of the molecule. It has been noted that increasing the conjugated system and adding electron donating groups can result in the bathochromic (red) shifting of the fluorescent spectra of dyes.[6]

The spectra, especially the excitation and emission maxima, of a dye are important to its effectiveness and usefulness. Dyes with unique or red-shifted emission spectra are sought after because they are less likely to cause spectral overlap in complex multi-stain studies. A fluorescent compound always has an emission that differs from its excitation.[8] This is important because without this difference, the intensity of emission would be impossible to differentiate from the excitation. [8] The difference between the excitation and emission maxima is known as the Stokes shift, named after Sir George Stokes.[6] Although dyes with small Stokes shifts of 20-40 nm have typically been used for biomedical research in the past, these small shifts are undesirable.[9] Re-excitation and high background signal can occur in dyes with small Stokes shifts due to the similarity of their excitation and emission spectra.[9] This re-excitation can produce a halo effect when utilizing high resolution stimulated emission depletion (STED) microscopy.[9] A small Stokes shift is also one of the primary reasons for self-quenching, resulting in a decrease in the brightness and quantum yield of a fluorophore.[1] Consequently, dyes with large Stokes shift ($\geq$ 70 nm) are desired because of their ability to more easily be utilized for super-resolution optical microscopy.[9, 10] A number of dyes have been synthesized with the purpose of having large Stokes shifts, but difficulties in producing these dyes have been noted. [10] Complex structures requiring lengthy multi-step reactions that produce a low yield of product have often been identified.[10]

Another important characteristic of a dye is its quantum yield, which demonstrates the effectiveness of a fluorophore by comparing the ratio of photons absorbed to those emitted by the fluorophore.[6] The photostability of a dye also contributes to its effectiveness and usefulness as a cell stain. This characteristic describes a dye's ability to maintain fluorescent properties after continued exposure to light. Other factors, such as changes in pH, have also been noted and exploited for their ability to impact fluorescence.[6]

Anthraquinones as Fluorescent DNA Dyes

Because fluorescence is typically found in aromatic molecules, anthraquinone derivatives are known as common fluorophores.[1] The structure of anthraquinones also lends itself to intercalate between DNA. A common feature of nearly all intercalating agents is a planar structure with polyaromatic systems, and anthraquinones are no exception.[11] These structural elements contributing to high DNA affinity are also seen in cell-permeable anthracycline antibiotics.[12] These characteristics contribute to the effectiveness of anthraquinones as fluorescent DNA binding dyes. Anthraquinone-derived dyes, such as DRAQ5, also exhibit high photostability. Although the anthraquinone core by itself does not display notably high photostability, the addition of substituents can greatly improve stability.[2] Some examples of commercially available anthraquinone dyes are DRAQ5, DRAQ7, and CyTRAK Orange. DRAQ5 is the most relevant due to its structural similarity to the proposed new compounds (Figure 2). While not all anthraquinones possess fluorescence, it is a common trait. Some anthraquinone-based drugs, such as mitoxantrone, even possess weak fluorescence.[13]

DRAQ5

DRAQ5 (Figure 2; Deep Red Anthraquinone 5) is a far-red fluorescing DNA-specific bisalkylaminoanthraquinone.[12] It is highly cell permeable (both plasma and nuclear membranes) and is effective at staining both live and fixed cells.[12] Although there are many DNA stains, DRAQ5 is one of a select few that is suitable for live cell studies.[14] DRAQ5 has also been found to be effective at discriminating between human leukocytes and lymphoma cells via flow cytometry.[15] The excitation maximum of DRAQ5 is 646 nm and the emission maximum is 681 nm.[12] The intercalation of DRAQ5 into DNA shifts the emission maxima towards 697 nm.[12] Due to DRAQ5's far-red fluorescence emission, it is able to fluoresce with less overlap from other commercially popular fluorophores excitable via UV and visible light.[12] Its far-red emission spectra is a desirable property. However, DRAQ5 demonstrates high levels of chemical cytotoxicity, a small Stokes shift (less than 30 nm), and a low quantum yield of 0.003 in solution.[14, 16] It possesses a high photostability.[17]

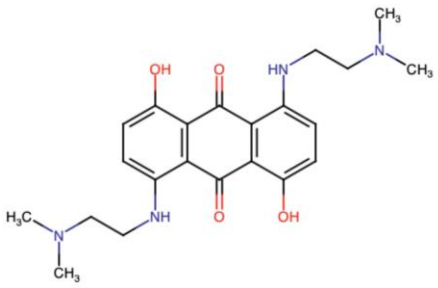

Figure 2. Structure of DRAQ5.

DRAQ5 has been found to both intercalate and bind to the minor groove of DNA, especially to A-T sequences. This biomechanistic interaction of DNA has been determined to be concentration dependent; at low concentrations of less than 0.5 µM DRAQ5, the dye acts as a minor groove binder, while at high concentrations of more than 0.5 µM, DRAQ5 intercalates

between the planar bases of DNA.[18]

DRAQ7

DRAQ7 is chemically derived from DRAQ5 but exhibits different features. While DRAQ5 exhibits high cytotoxicity, DRAQ7 does not due to its inability to penetrate the plasma membrane of living cells.[19] It instead only intercalates into the DNA of dead or permeabilized cells. [20] This allows DRAQ7 to provide real-time data in cell viability assays.[19] It has excitation and emission peaks of 599/644 nm and 678/697 nm, respectively.[21] The structure of DRAQ7 is currently proprietary.

CyTRAK Orange

CyTRAK Orange is a fluorescent dye derived from a chemical modification of DRAQ5.[17] Instead of a high nuclear specificity like DRAQ5, CyTRAK Orange binds at higher rates to cytoplasmic RNA.[17] This characteristic, in addition to its cell permeability in both live and fixed cells, allows the dye to act as a counterstain by highlighting the cytoplasm.[17] It has an absorption maximum at 510 nm and an excitation maximum at 610 nm.[17] There is currently no available structure for this dye.

Non-Anthraquinone Fluorescent DNA Dyes.

Although anthraquinone fluorescent dyes are useful, they are certainly not the most commonly used or readily available for biomedical applications. Certain individual dyes, such as DAPI and propidium iodide, as well as families of dyes, including cyanine and rhodamine, are among the most popular. Because a perfect cell stain does not exist, only more or less ideal, each of these individual and groups of dyes have different pros and cons. The following dyes were selected for analysis in this literature review due to characteristics that could potentially compare

and contrast with the proposed new compounds. These characteristics include their photophysical qualities (dyes with excitation/emission from across the UV-vis spectrum were chosen), cell permeability, and usefulness for various analytical techniques.

DAPI

The blue dye DAPI (Figure 3; 4',6-diamidino-2-phenylindole) is a widely used cell permeable stain from the indol family of dyes commonly used for nuclear visualization in fluorescence and confocal microscopy.[18, 22] It excites in the UVA region at ~360 nm, has a broad emission spectrum with peaks at 454 nm and 437 nm, and has a resulting Stokes shift of 90 nm.[22] It has a high quantum yield of 0.92 when bound to double-stranded DNA.[23] DAPI can be utilized in conjunction with green fluorescent protein (GFP) and other green exciting dyes because it does not excite past 450 nm.[24] DAPI demonstrates poor photostability, with photobleaching evident in as little as 2 minutes of exposure to 405 nm or ultraviolet light.[24] It has been found that UV exposure causes protonation of the dye.[22] This high level of photobleaching limits the dye's usefulness for longer term techniques such as cell tracking. The UV excitation also limits its use for live cell imaging, because it can lead to cell death.[18]

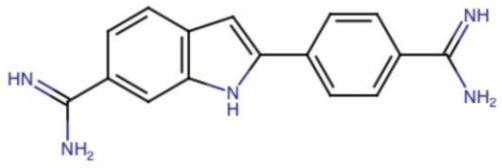

Figure 3. Structure of DAPI.

DAPI interacts with DNA by acting as a minor groove binder via electrostatic forces and hydrogen bonding. The dye binds with a higher specificity to A-T base pairs.[25] Upon DNA binding, the fluorescence of DAPI increases 20 times.[24]

Propidium Iodide

Propidium iodide (Figure 4; PI) is a widely used cell impermeant red-fluorescing nuclear dye.[26] Due to its ability to solely stain dead cells, specifically those with compromised membranes, it is commonly used in cell staining and flow cytometry to evaluate apoptosis and cell viability.[26, 27] The excitation and emission peaks of PI dissolved in water are 495 nm and 619 nm, respectively, with a resulting large Stokes shift of 124 nm.[28] PI is documented as having high quantum yield and good photostability.[29]

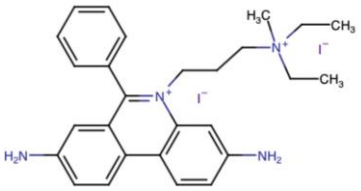

Figure 4. Structure of propidium iodide.

Propidium iodide binds to nucleic acids via intercalation.[28] It binds stoichiometrically to both DNA and RNA with no preference for specific sequences.[26, 27] Thus, brightness of the fluorescence of PI depends on the ratio of the dye to nucleic acids in the sample.[26] Due to the non-specificity for nucleic acids, it is important to treat cells with nucleases prior to staining.[30] Similar to DAPI, the fluorescence of PI increases 20 to 30 times upon interaction with DNA.[26]

Cyanine

Initially used in color photography, the cyanine family of dyes (Figure 5) are fluorescent molecules containing a chain of conjugated double bonds that link the nitrogen atoms of two heterocyclic structures.[31] This family of dyes have become extremely popular DNA dyes, to the point where the current majority of commercially available fluorescent DNA stains are cyanines.[32] The excitation and emission maxima of cyanine dyes are 789 nm and 817 nm,

respectively, resulting in a small Stokes shift of 28 nm.[6] The quantum yield of cyanine dyes is typically 0.05.[6] Poor photostability is often characteristic of cyanine dyes, especially those designed to be excited by near-infrared light. [33]

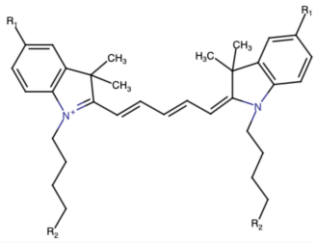

Figure 5. Structure of cyanine. The R groups demonstrate the most common sites for functional group addition.

Both cell-permeant and impermeant cyanine dyes are available for use in techniques such as DNA visualization assays and fluorescence microscopy.[34] Cyanine dyes can act as both DNA intercalators as well as groove binders.[32] The heterocyclic nitrogen-containing structures allow intercalation between DNA base pairs while the chain of conjugated double bonds, a polymethine bridge, is flexible enough to allow binding to the minor groove of DNA.

Rhodamine

Rhodamine (Figure 6) constitutes a family of dyes, itself being a subset of xanthenes, that are popular fluorescent probes due to their photophysical properties and compatibility with biological systems.[1] They are known for possessing high photostability, resistance to photobleaching, and high quantum yields.[1] It has also been found that the addition of different substituents at the R groups seen in Figure 6, specifically alkyl substituents, can cause characteristics such as quantum yield to be impacted with changes in temperature.[35] This trait gives the dye additional biomedical use as a fluorescent optical thermometer.[35] The excitation and emission maxima of rhodamine are 512 nm and 530 nm, respectively.[6] Consequently,

rhodamine dyes normally demonstrate undesirable small Stokes shifts of 18 nm.[6]

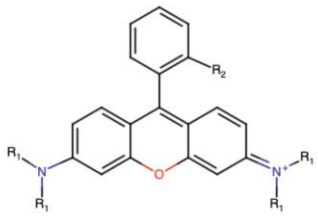

Figure 6. Structure of rhodamine. R groups 1-4 demonstrate the typical positions for functional groups added to rhodamine dyes.

Rhodamine dyes, such as Rhodamine 123, are cell permeable.[36] R123 in particular is transported into cells via passive and active means.[36] Once in the cell, rhodamine dyes, such as Rhodamine B, interact with DNA as a groove binder.[37]

Comparison of Anthraquinone and Non-Anthraquinone Dyes

Although non-anthraquinone dyes are more commonly used in research laboratories around the world, it is not necessarily because they are superior. Fluorescent dyes possessing different cores each have their own advantages and drawbacks (Table 1). Anthraquinones, such as DRAQ5 and CyTRAK Orange, tend to possess high chemical stability and photostability.[17] Many popular non-anthraquinone dyes, such as DAPI and cyanine, exhibit poor photostability.[24, 33] While DAPI demonstrates photobleaching within 2 minutes, DRAQ5 is much more stable. Other non-anthraquinones, such as Rhodamines, possess higher photostability. However, this comes at a drawback of possessing small Stokes shifts. Thus, although rhodamine is photostable and can be used for cell tracking, it can exhibit high background interference and self-quenching. This is important because dyes that demonstrate large Stokes shifts are highly sought after due to their use in super-resolution optical microscopy.[9] It is important to note that DRAQ5 does not have a large Stokes shift, but both DRAQ7 and CyTRAK Orange have shifts greater than 70 nm.

Thus, fluorescent photostable anthraquinones may possess either large or small Stokes shifts.

Table 1. Comparison of Photophysical and Staining Characteristics of Anthraquinone and Non-Anthraquinone Compounds

Compound	DRAQ5	DRAQ7	CyTRAK Orange	DAPI	Propidium Iodide	Cyanine	Rhodamine
Excitation (nm)	646	599/644	510	~360	495	789	512
Emission (nm)	681	678/697	610	437/454	619	817	530
Stokes Shift (nm)	35	79	100	90	124	28	18
Quantum Yield	.003	N/A	N/A	High	High	.05	.86
Permeability	Yes	No	Yes	Yes	No	Both	Yes
Photostability	High	High	High	Poor	High	Poor	High
DNA Binding	Both	Intercalator	Intercalator	Groove Binder	Intercalator	Both	Groove Binder

Anthraquinones as Antimicrobial and Chemotherapeutic Agents

The continual search for cancer therapies has led scientists to the discovery that a number of anthraquinone derivatives exhibit promising characteristics relating to autophagy. Mitoxantrone is a common anthraquinone-based drug used either alone or with other forms of chemotherapy to treat a wide variety of cancers (Figure 7A).[38]

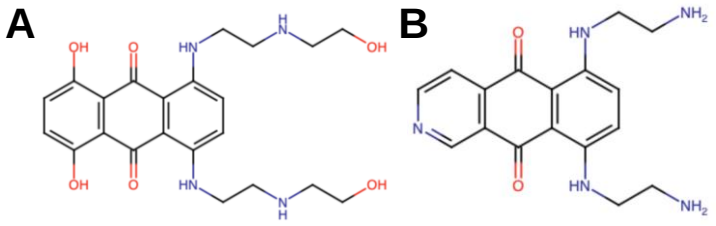

Figure 7. Structures of mitoxantrone (A) and pixantrone (B).

The planar nature of mitoxantrone along with its functional groups allow it to act as both a dsDNA intercalator and groove binder depending on the level of concentration.[18] This DNA binding mechanism prevents the enzyme DNA topoisomerase II from properly relaxing the DNA

supercoils, thus inhibiting DNA replication.[39] Interestingly, mitoxantrone demonstrates weak fluorescence, with excitation and emission maxima at 610/685 nm, respectively.[13] Other chemotherapeutic anthraquinone-based agents include pixantrone and anthracyclines (Figure 7B). Based on the similarity of structures, it is possible that our proposed new DNA binders could have a similar effect of cytotoxicity. By preventing DNA replication, the compounds could induce autophagy and function as a form of antitumor therapy. Mitoxantrone, aclarubicin, and doxorubicin are all prime examples of anthraquinone-derived antitumor drugs.[40]

Some anthraquinone derivatives have also been identified as antimicrobial compounds. For example, the molecules ranjidiol, rubiadin, and damnacanthal were naturally derived from *Heterophyllaea pustulata*, a species of shrub, and exhibited antibacterial activity against *Staphylococcus aureus*.[5] Thus, anthraquinone-derived molecules have been found to possess a wide range of biomedical uses.

■ RESULTS

Synthesis and Characterization of Anthraquinone Compounds

Several compounds were synthesized from an anthraquinone core. Functional groups were potentially added onto one or more of the R groups evident in Figure 8.

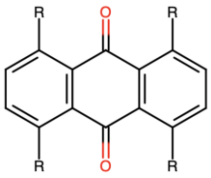

Figure 8. Anthraquinone core with potential R groups used for new compounds.

Although the precise substituents cannot be revealed due to the sensitive nature of the work, they are unique and were chosen with the goal of increasing cell permeability and adding desirable photophysical characteristics.

1. RBS1

RBS1 was synthesized, and its analysis showed that it was different from its starting reagents. Crop 1 and 2 of RBS1 demonstrate a single impurity according to thin layer chromatography (TLC) results, but the infrared spectroscopy (IR) indicates that the compound is different compared to the starting reagent. The melting points (m. p.) of the recrystallized products are different from the original product and are higher and less wide, though the first crop has a wider m. p. than the original. The IR also demonstrates that crops 1 and 2 are similar, yet different from the starting reagent. The rf values of the TLCs demonstrate that RBS1 is different from the starting reagent and that the two recrystallizations of RBS1 have the same rf value. One impurity with a high rf value remains in the TLC. NMR analysis indicated a high level of purity in crop 2 of RBS1. The characteristic NMR features point to the proper structure of the desired product. A ^{13}C-NMR, demonstrated the expected number of carbons.

Melting Point

The melting point of crude RBS1 was found to be 153.6-154.2 ^{o}C. After recrystallization, the melting point of crop 1 was 163.8-165.5 ^{o}C and crop 2 was 169.6-170.3 ^{o}C.

Amount of Product

11.603 grams of RBS1 was initially produced. After recrystallization, a total sum of all crops of 10.028 g was recovered (88.2% yield).

TLC

RBS1 was analyzed via TLC with silica gel as the stationary phase (Figure 9). The mobile phase was a mixture of ethyl acetate: hexanes (7:3). The reagent (1) and product (3) were dissolved in acetone.

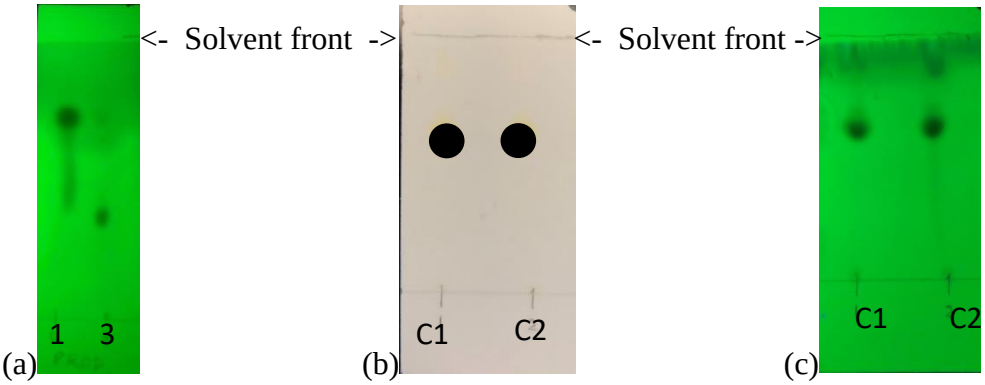

Figure 9. TLC analyses of RBS1. (a) A TLC of **1** and **3** with ethyl acetate: hexanes (7:3) as mobile phase. (b and c) A TLC conducted to compare crops 1 and 2 (in lanes C1 and C2, respectively); (b) is under visible light and (c) is under short-wave UV light (254 nm).

The rf values for starting material 1 and RBS1 were 0.74 and 0.35, respectively (Figure 9a). There appeared to be a slight contamination of reagent **1** in product **3** at an rf value of 0.74; yet, a high concentration of a new product was synthesized. After recrystallization of RBS1, a TLC was conducted to compare the purity of crops 1 and 2. Silica gel was used as the stationary phase. The rf values of both spots were 0.63. A minor impurity was detected in lane C2 with an rf value of 0.87. The rf values for **3** differ between (a) and (c) because a slightly different mobile phase was used**.** Thus, the synthesized RBS1 product **3** is different from **1.**

2. RBS3

RBS3 was synthesized with RBS1 as a reagent.

Appearance

Initially, no fluorescence was observed. However, after further workup, it was found to fluoresce.

Amount of Product

The precise amount of product RBS3 is unknown. Although 0.114 g of RBS1 was used

for the reaction, the yield is unknown until further work is done.

TLC

The product RBS3 was analyzed via TLC with silica gel as the stationary phase. (Figure 10) The mobile phase was a mixture of ethyl acetate: hexanes (7:3). The TLC was placed under short-wave UV light (254 nm). The TLC confirms successful modification because a new spot with a different rf value compared to RBS1, 0.00 instead of 0.63, was formed. Two minor impurities were also found, with rf values of 0.12 and 1.00, respectively.

Figure 10. A TLC of **3** with ethyl acetate: hexanes (7:3) as mobile phase was made. The TLC is under short-wave UV light (254 nm). Silica gel was used as the stationary phase.

3. CE8 and NGA5

Compounds NGA5 and CE8 were synthesized by Nicholas Aboreden (presently at the University of Pennsylvania) and Connor Ellis (presently at Liberty University College of Osteopathic Medicine).

Fluorescence Spectra of Anthraquinone Compounds

Three compounds, RBS3, CE8, and NGA5, were dissolved in deionized water and analyzed for their excitation and emission spectra.

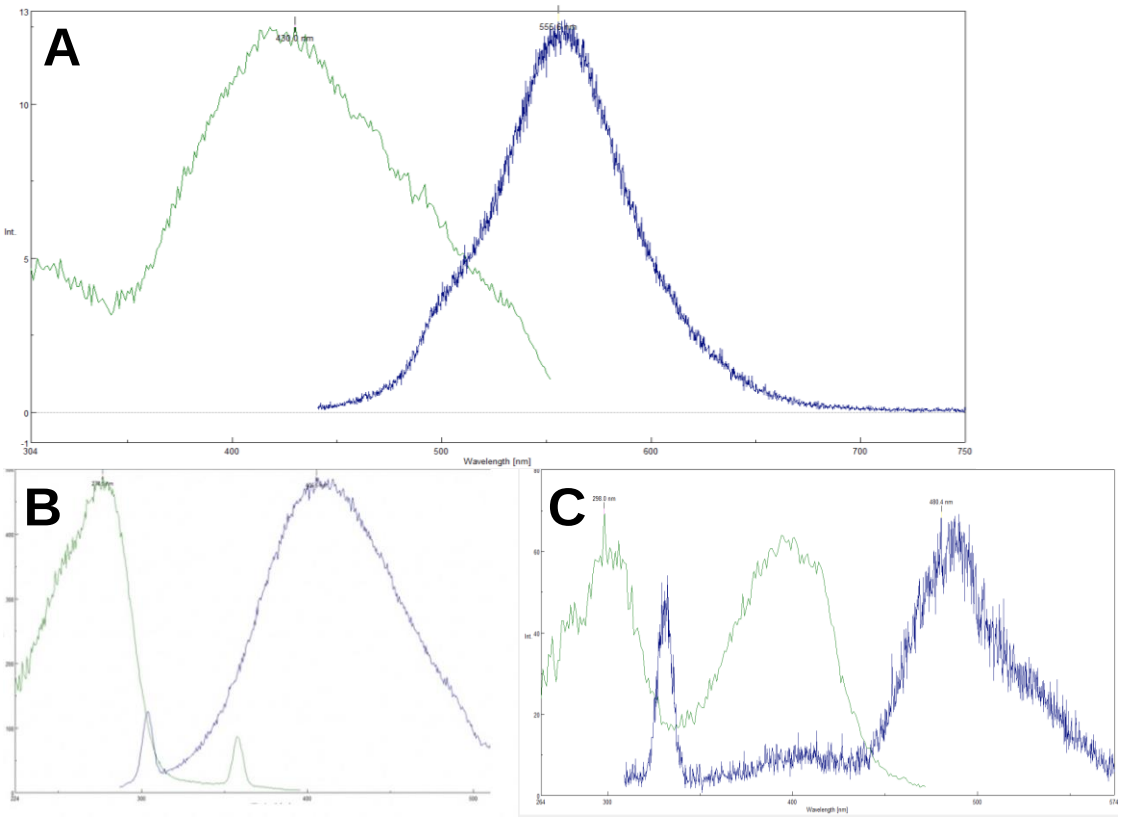

Figure 11. Excitation and emission spectra of anthraquinone derivatives in deionized water. 11A shows the spectra of RBS3, with an excitation maximum of 420 nm, and an emission maximum of 556 nm. 11B displays the spectra of CE8. Excitation and emission peaks were recorded at 276 nm and 406 nm, respectively. Sub-optimal excitation and emission peaks were also recorded at 300 nm and 360 nm, respectively. This finding is unusual and needs further investigation. 11C shows the spectra of NGA5. Its excitation/emission maxima are 298/480 nm, with additional excitation/emission peaks at 400/325 nm, respectively.

Biomedical Testing of Anthraquinone Compounds

It is vital when synthesizing new fluorescent dyes and chemotherapeutic agents that the desired compound is of high purity. Impurities can inhibit the efficiency of the compound and cause unwanted harm to living cells. The apparent purities of RBS1 and RBS3 are promising but

further analysis should be done to ensure a purity of 99% for potential commercial use.

A variety of biomedical analyses were performed to characterize the usefulness of the new compounds. Fixed tissue staining and fixed and live cell staining were conducted and visualized with fluorescence microscopy. Flow cytometry will be conducted in the future. The new compounds may also demonstrate antimicrobial potency. It is impossible to know for certain without further analysis, but the structural similarities between the new compounds and commercially available dyes and drugs imply potential uses in these areas.

Staining Fixed and Live Cells

RBS3. The staining effectiveness of RBS3 with fixed and live cells was examined at various concentrations. In an attempt to identify precisely what structures are stained by the dye, RBS3 was compared to established cell stains. These included nuclear stain DAPI and endoplasmic reticulum stain ERTracker Green.

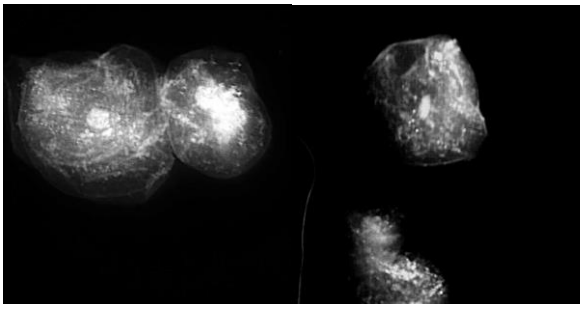

Figure 13. Methanol/acetone fixed buccal epithelial cells stained with 1 mM RBS3.

The slides were immersed in a 1:1 solution of methanol and acetone, and then incubated in a freezer for 20 minutes. Then, the cells were washed with 1X PBS and immersed in the dye for 15 minutes. All stained cells exhibited nuclear, cytoplasmic, and puncta-like staining.

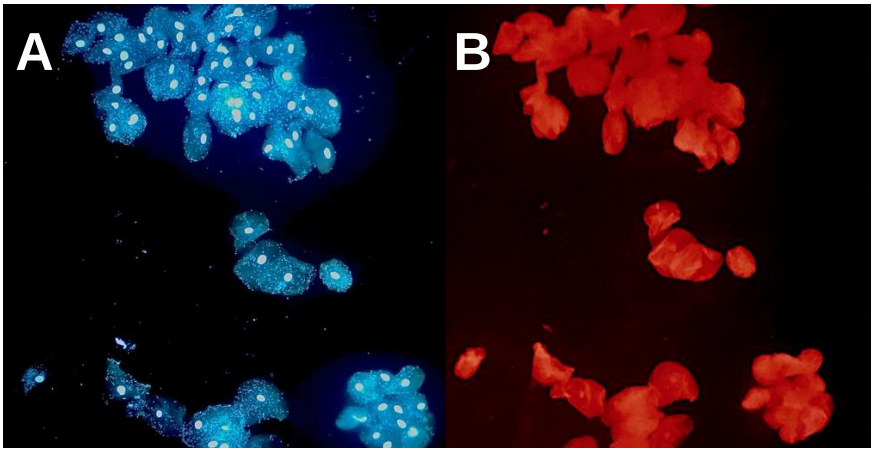

Figure 14. Acetone fixed buccal epithelial cells stained with 0.5 mM RBS3 and 0.18 mM DAPI. 14A was taken using the DAPI preset filter and 14B was taken using the rhodamine preset filter on the fluorescence microscope.

Cells were fixed with 100% acetone and incubated in the freezer for 20 minutes. Then, the cells were washed with 1X PBS and incubated with RBS3 and DAPI for 10 minutes. The nuclei of the cells can be seen in 14A, but unless proven otherwise, it is due to DAPI. The concentration of DAPI was higher than the recommended protocol, so this procedure should be conducted again with lower concentrations of both dyes.

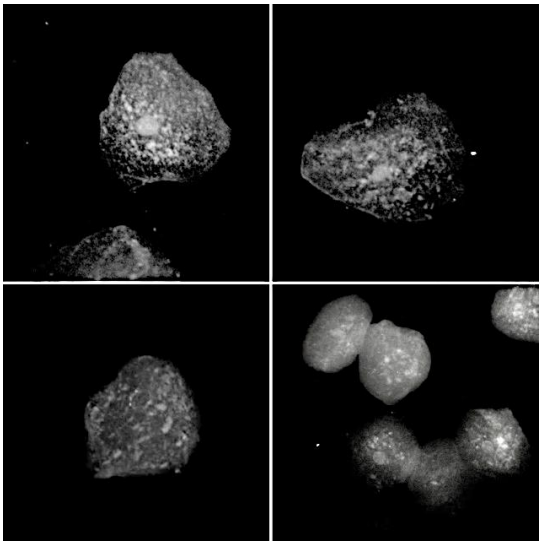

Figure 15. Buccal epithelial cells stained with 20 µM RBS3 incubated for 48 hours at room temperature. A DAPI preset filter was used to obtain the images.

Some nuclear specificity is evident. High specificity for asymmetrical vesicles localized around the nucleus and unspecified puncta is also evident.

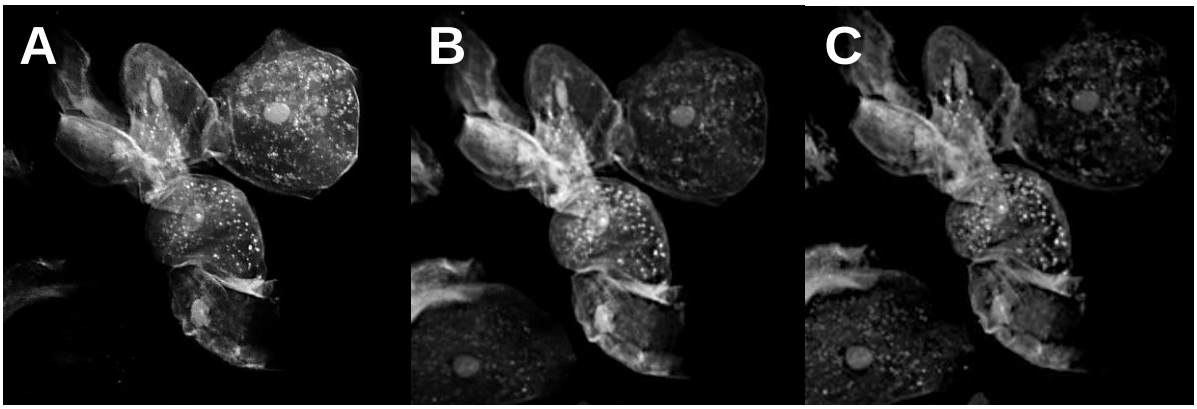

Figure 16. Live buccal epithelial cells stained with 100 µM RBS3. 16A, 16B, and 16C were imaged with DAPI, Rhodamine, and Fluor preset filters, respectively.

The cells were incubated in 1X PBS at room temperature for 20 minutes. No washing step was required for imaging. RBS3 intensely stained small puncta throughout the cells. All stained cells also exhibited cytoplasmic staining and some nuclear staining.

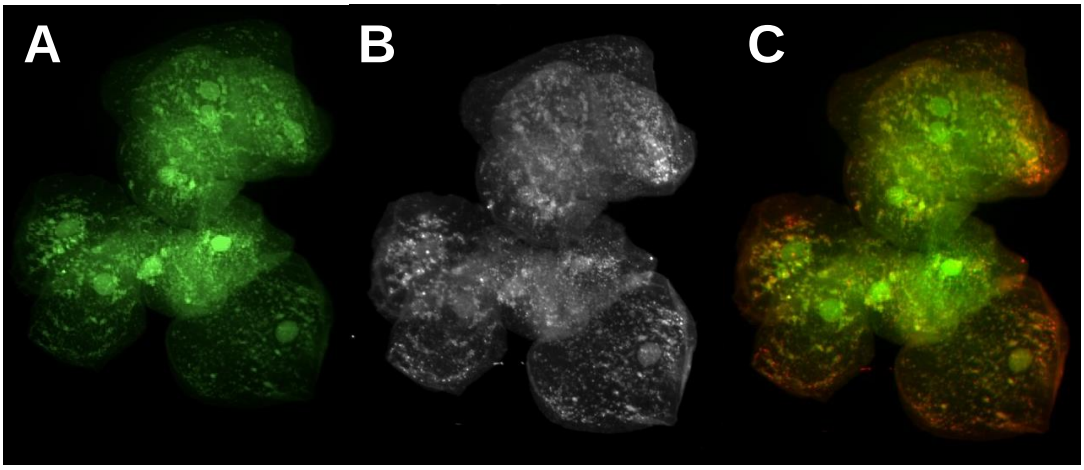

Figure 17. Comparison of ERTracker Green and RBS3 staining live buccal epithelial cells. (A) is 1 µM ERTracker Green, a fluorescent dye selective for staining endoplasmic reticulum, imaged with the FITC filter, (B) is 100 µM RBS3 imaged using the DAPI preset filter after 30 minutes exposure to light. (C) is a merged image with RBS3 in the red channel and ERTracker Green in the green channel.

The yellow portions of the merged image 17C show the overlap between the ERTracker Green and RBS3. Nearly all stained structures overlapped with both the ERTracker Green and RBS3 dyes. Notable exceptions to this include several small, intensely stained puncta near the cell membrane highlighted by RBS3, and more intensely stained nuclei with ERTracker Green.

Antimicrobial Analysis

A Kirby-Bauer test was conducted on each of the three anthraquinone derivates in triplicate according to protocol (Table 2). Both gram positive (*S. aureus*) and gram negative (*E. coli*) bacteria were tested.

Table 2. Kirby Bauer Test of the three anthraquinone derivatives and a positive control.

	+ control (Lysol)	1 mM RBS3	1 mM NGA5	1 mM CE8
E. Coli diameter (mm)	13, 15, 16	10, 8, 8	0, 0, 0	9, 6, 0
S. aureus diameter (mm)	24, 22, 23	0, 0, 0	0, 0, 0	16, 7, 0

■ DISCUSSION

Fluorescence Spectra of Anthraquinone Compounds

The fluorescence spectra of the synthesized compounds exhibited promising results. The emission spectra of RBS3 demonstrated a Stokes shift of roughly 136 nm, CE8 demonstrated a Stokes shift of 130 nm, and NGA5 exhibited a Stokes shift of 80 nm, with a minor Stokes shift of 27 nm also evident due to two excitation/emission peaks. This finding is especially important for fluorescent dyes because larger Stoke shifts allow for higher resolution microscopy and eliminates fluorescence quenching by reducing absorption and emission overlap. The novel dyes have a larger Stokes shift compared to that of their direct anthraquinone competitors, such as DRAQ5, as well as non-anthraquinone competitors. Both DRAQ5 and DRAQ7 have a Stokes shift of 62 nm. DAPI has a fairly sized Stokes shift of 98 nm, but two of the synthesized compounds still had larger shifts. These large Stokes shifts are particularly of note because the syntheses, especially for RBS3, are relatively simple. This is important because it has been documented that dyes with large Stokes shifts typically require complex reactions resulting in low yields.[10] The new cell stain RBS3 appears to be more photostable than some non-anthraquinone fluorophores, such as DAPI and ERTracker Green, and comparable to DRAQ5 based on rudimentary observation of photostability (Figure 17). Based on these results, the new

dyes have distinct and valuable photophysical characteristics.

Biomedical Testing of Anthraquinone Compounds

Staining Fixed and Live Cells

The staining of both fixed and live cells proved to be successful with RBS3. Fixed staining of buccal epithelial cells using methanol: acetone (1:1) effectively stained the cells and was excitable using the DAPI and Rhodamine filters (Figure 14). Live cell staining (Figure 16) also showed effective staining and imaging, even without a washing step. Thus, RBS3 is highly cell permeable. Based on initial oversaturated cytoplasmic staining, much lower concentrations (20 µM and 100 µM) were later used (Figures 15 and 16). It was also noted that the cells still maintained fluorescence even after 30 minutes to an hour of exposure to light, demonstrating a resistance to photobleaching. Surprisingly, RBS3 gradually fluoresced brighter several minutes after initial exposure to light.

A noticeable characteristic of the RBS3 dye staining fixed and live cells was that it appeared to most intensely stain puncta-like vesicles dispersed throughout the cell and asymmetrical vesicles centralized around the nucleus (Figures 15 and 16). In the merged image Figure 17, it is clear that there is a high amount of overlap between the endoplasmic reticulum dye and the novel compound. Although the nuclei stained brighter with ERTracker Green, RBS3 exhibited nearly a complete overlap of all structures highlighted by the ER dye. However, the intensity of the red channel in other spots indicates that RBS3 may also be staining additional structures. Interestingly, the most intensely stained red spots appear to be puncta near the plasma membrane of the cells. Based on this information, it is possible that RBS3 is staining organelles of the endomembrane system. RBS3 may bind to or accumulate in vesicles, the ER, and other

organelles of this system. More research should be conducted on this topic. Staining with other commercial dyes, such as MitoTracker Red, was conducted, but did not demonstrate the highly similar staining seen in Figure 17.

Based on Figures 13, 16, and 17, RBS3 is cell permeable, does not require a wash step, and stains the endoplasmic reticulum. RBS3 also stains the cytoplasm, nucleus, and other unidentified vesicles with varying specificity. Dyes CE8 and NGA5 require further investigation into their use for cell staining.

Antimicrobial Analysis

The Kirby-Bauer disc diffusion test revealed that the compounds possess minor to no antimicrobial activity. NGA5 showed no antibacterial activity, CE8 showed minor antibacterial activity on both types of bacteria, and RBS3 showed minor antibacterial activity against gram negative bacteria.

■ CONCLUSIONS

In summary, three new anthraquinone-derived fluorescent compounds were produced that possess large Stokes shifts. One of the compounds, RBS3, demonstrates potential use as a fluorescent cell stain. RBS3 is highly cell permeable, appears to be resistant to photobleaching, does not require any wash-off for imaging, and stains the cytoplasm, nucleus, endoplasmic reticulum, and other puncta-like vesicles. Based on these results, it is possible that RBS3 stains organelles of the endomembrane system by binding to or accumulating in vesicles of the system. Additionally, RBS3 provides an example of a large Stokes shift dye that, unlike many others, requires a relatively simple synthesis and structure. This characteristic may allow RBS3 to act as an inexpensive and effective alternative fluorophore for high resolution fluorescence

microscopy. Additional examination of its synthesis and characteristics could potentially provide insight into synthesizing simpler and inexpensive dyes with large Stokes shifts.

■ EXPERIMENTAL SECTION

General Methods. All commercial chemicals were used without purification.

Physical Characterization. TLC stationary phase (Selecto Scientific) was used as received. The melting points were analyzed using a Digimelt SRS, the IR instrument used was a FT-IR Spectrometer model Spectrum Two (Perkin Elmer), and a 400 MHz JEOL FT-NMR spectrometer with multi-nuclear probe was used (Longwood University).

Fluorescence Spectra. A Jasco FP-8300 Spectrofluorometer with quartz cuvettes was used.

Obtaining and preparing cheek cells. Buccal epithelial cells were harvested by swabbing the inside of the cheek and the maxillary and mandibular buccal sulcus for 10 seconds with a sterile, cotton tipped applicator. This applicator was then washed in a 1X PBS solution. The solution was subsequently treated with the various stains. Wet-mount slides were prepared using this solution.

Fluorescence Microscopy Imaging. Buccal epithelial cells were used for both live and fixed cell staining with a Zeiss Axioskop 2 Plus fluorescence microscope. DAPI (Thermo Fisher #62248) and ERTracker Green (Thermo Fisher #E34251) staining were followed according to established protocol.

Antimicrobial Analysis. A Kirby-Bauer test was conducted on TSA plates streaked with *E. coli* and *S. aureus*. The discs were dipped in 1 mM anthraquinone derivatives dissolved in 1X PBS. Lysol was used as a positive control. The plates were incubated for 48 hours at 37 ^{o}C.

References

(1) Gong, J.; Liu, C.; Jiao, X.; He, S.; Zhao, L.; Zeng, X. *RSC Adv.* **2020**, *10*, 38038-38044.

(2) Chang, I. Y.; Miller, I. K. *Journal of the Society of Dyers and Colourists* **1986**, *102*, 46-53.

(3) Huang, L.; Zhang, T.; Li, S.; Duan, J.; Ye, F.; Li, H.; She, Z.; Gao, G.; Yang, X. *PLOS ONE* **2014**, *9*, e108286.

(4) Deitersen, J.; El-Kashef, D. H.; Proksch, P.; Stork, B. *Bioorg. Med. Chem.* **2019**, *27*, 115042.

(5) Comini, L. R.; Núñez Montoya, S. C.; Páez, P. L.; Argüello, G. A.; Albesa, I.; Cabrera, J. L. *Journal of Photochemistry and Photobiology B: Biology* **2011**, *102*, 108-114.

(6) Jun, J. V.; Chenoweth, D. M.; Petersson, E. J. *Org. Biomol. Chem.* **2020**, *18*, 5747-5763.

(7) Lakowicz, J. R. In *Principles of Fluorescence Spectroscopy;* Springer US: Boston, MA, 2006.

(8) Fu, Y.; Finney, N. S. *RSC Adv.* **2018**, *8*, 29051-29061.

(9) Sednev, M. V.; Belov, V. N.; Hell, S. W. *Methods and Applications in Fluorescence* **2015**, *3*, 042004.

(10) Gao, Z.; Hao, Y.; Zheng, M.; Chen, Y. *RSC Adv.* **2017**, *7*, 7604-7609.

(11) Adhikari, A.; Mahar, A. S. *Int J Pharm Pharm Sci* **2016**, *8*, 17-25.

(12) Smith, P. J.; Blunt, N.; Wiltshire, M.; Hoy, T.; Teesdale-Spittle, P.; Craven, M. R.; Watson, J. V.; Amos, W. B.; Errington, R. J.; Patterson, L. H. *Cytometry* **2000**, *40*, 280-291.

(13) Bell, D. H. *Biochimica et Biophysica Acta (BBA) - Gene Structure and Expression* **1988**, *949*, 132-137.

(14) Zhang, S.; Fan, J.; Li, Z.; Hao, N.; Cao, J.; Wu, T.; Wang, J.; Peng, X. *J. Mater. Chem. B* **2014**, *2*, 2688-2693.

(15) Smith, P. J.; Wiltshire, M.; Davies, S.; Patterson, L. H.; Hoy, T. *J. Immunol. Methods* **1999**, *229*, 131-139.

(16) Njoh, K. L.; Patterson, L. H.; Zloh, M.; Wiltshire, M.; Fisher, J.; Chappell, S.; Ameer-Beg, S.; Bai, Y.; Matthews, D.; Errington, R. J.; Smith, P. J. *Cytometry* **2006**, *69A*, 805-814.

(17) Edward, R. *Mol. Cells* **2009**, *27*, 391-396.

(18) Wang, Y.; Schellenberg, H.; Walhorn, V.; Toensing, K.; Anselmetti, D. *Materials Today: Proceedings* **2017**, *4*, S218-S225.

(19) Akagi, J.; Kordon, M.; Zhao, H.; Matuszek, A.; Dobrucki, J.; Errington, R.; Smith, P. J.; Takeda, K.; Darzynkiewicz, Z.; Wlodkowic, D. *Cytometry* **2013**, *83A*, 227-234.

(20) Anonymous. DRAQ7™ (ab109202). *https://www.abcam.com/draq7trade-ab109202.html?productWallTab=ShowAll*.

(21) Anonymous. DRAQ7™ Dye. *https://www.thermofisher.com/order/catalog/product/D15106?us&en#/D15106?us&en*.

(22) Żurek-Biesiada, D.; Kędracka-Krok, S.; Dobrucki, J. W. *Cytometry* **2013**, *83A*, 441-451.

(23) Estandarte, A. K.; Botchway, S.; Lynch, C.; Yusuf, M.; Robinson, I. *Scientific reports* **2016**, *6*, 31417.

(24) Piterburg, M.; Panet, H.; Weiss, A. *J. Microsc.* **2012**, *246*, 89-95.

(25) Gryczynski, I.; Malak, H.; Lakowicz, J. R. *Bioimaging* **1996**, *4*, 138-148.

(26) Riccardi, C.; Nicoletti, I. *Nature Protocols* **2006**, *1*, 1458-1461.

(27) Stiefel, P.; Schmidt-Emrich, S.; Maniura-Weber, K.; Ren, Q. *BMC microbiology* **2015**, *15*, 36.

(28) Samanta, A.; Paul, B. K.; Guchhait, N. *Journal of Photochemistry and Photobiology B: Biology* **2012**, *109*, 58-67.

(29) Poulin, N. M.; Matthews, J. B.; Skov, K. A.; Palcic, B. *J. Histochem. Cytochem.* **1994**, *42*, 1149-1156.

(30) Rosenberg, M.; Azevedo, N. F.; Ivask, A. *Scientific reports* **2019**, *9*, 6483.

(31) Saccone, D.; Galliano, S.; Barbero, N.; Quagliotto, P.; Viscardi, G.; Barolo, C. *Eur. J. Org. Chem.* **2016**, *2016*, 2244-2259.

(32) Biver, T.; De Biasi, A.; Secco, F.; Venturini, M.; Yarmoluk, S. *Biophys. J.* **2005**, *89*, 374-383.

(33) Bera, A.; Bagchi, D.; Pal, S. K. *J Phys Chem A* **2019**, *123*, 7550-7557.

(34) Anonymous. Nucleic Acid Stains - Section 8.1. *https://www.thermofisher.com/us/en/home/references/molecular-probes-the-handbook/nucleic-acid-detection-and-genomics-technology/nucleic-acid-stains.html#head1*.

(35) Moreau, D.; Lefort, C.; Burke, R.; Leveque, P.; O'Connor, R.,P. *Biomedical optics express* **2015**, *6*, 4105-4117.

(36) Forster, S.; Thumser, A. E.; Hood, S. R.; Plant, N. *PLOS ONE* **2012**, *7*, e33253.

(37) Islam, M. M.; Chakraborty, M.; Pandya, P.; Al Masum, A.; Gupta, N.; Mukhopadhyay, S. *Dyes and Pigments* **2013**, *99*, 412-422.

(38) Morreal, C. E.; Bernacki, R. J.; Hillman, M.; Atwood, A.; Cartonia, D. *J. Med. Chem.* **1990**, *33*, 490-492.

(39) Abu Saleh, M.; Solayman, M.; Hoque, M. M.; Khan, M. A. K.; Sarwar, M. G.; Halim, M. A. *BioMed Research International* **2016**, *2016*, 6817502.

(40) Malik, E. M.; Müller, C. E. *Med. Res. Rev.* **2016**, *36*, 705-748.